Selective oxidation of aqueous organic pollutants over MOFs-based catalysts: A mini review

Fu-Xue Wang [a,b], Zi-Chen Zhang [a,b], Chong-Chen Wang [a,b,*]

[a] Beijing Key Laboratory of Functional Materials for Building Structure and Environment Remediation, Beijing University of Civil Engineering and Architecture, Beijing 100044, PR China
[b] Beijing Energy Conservation & Sustainable Urban and Rural Development Provincial and Ministry Co-construction Collaboration Innovation Center, Beijing University of Civil Engineering and Architecture, Beijing 100044, PR China

ARTICLE INFO

ABSTRACT

Efficient decontamination from water have attracted global attention in recent years. Advanced oxidation processes (AOPs) are widely used for aqueous organic pollutants degradation for water purification. However, it still is great challenge to efficiently oxidize the trace micropollutants especially from sewage matrix containing complicated matters, which would consume the reactive species to inhibit the decomposition of the target contaminants. Recently, many researchers devoted to the selective oxidation to address the above-mentioned problem. Various environmental functional materials like metal oxides and carbonaceous materials have been applied as catalysts for selective organic pollutants oxidation. Among them, metal–organic frameworks (MOFs) and their composites/derivatives displayed huge potential due to their designable structure and excellent catalytic performance. This review presented the research progress of MOFs-based materials in selective oxidation toward aqueous organic pollutants, in which some examples were analyzed in detail to show their performances, mechanisms as well as influence factors. The unique advantages of MOFs-based materials for selective oxidation were also discussed. Finally, the challenges and prospects of MOFs-based environmental functional materials in selective oxidation from water were proposed.

1. Introduction

In recent decades, water quality has received widespread attention due to the continuously discharged emerging contaminants (ECs) like pharmaceuticals and personal care products (PPCPs), polychlorinated biphenyl (PCBs), pesticides, organic dyes and so on [1,2]. These contaminants are harmful to aquatic life and human being even at trace concentration (ng/L ~ μg/L). Unfortunately, due to their physico-chemical nature like low concentration and high toxicity, ECs could not be efficiently removed by conventional technologies such as adsorption and biological treatment [3].

Advanced oxidation processes (AOPs) could efficiently eliminate contaminants by the in-situ generated radicals (e.g. hydroxyl (•OH), superoxide radical (O_2^-), sulfate radical ($SO_4^{•-}$)), which have raised wide attention due to their easy operation, mild reaction conditions and high efficiency [4]. The radicals with high oxidation ability could not only directly decompose the organic pollutants, but also reduce their toxicity

and even mineralize them to CO_2 [5,6]. Various of AOPs, such as photocatalysis, Fenton/Fenton-like reaction, electrocatalysis, ozonation and their coupling technologies have been developed for water treatment in recent years [7–10]. Numerous efforts have been devoted to enhance oxidation efficiency. However, it was inhibited in actual application resulting from the complicated compositions in wastewater, in which the generated reactive oxygen radicals (ROSs) would be highly consumed by the co-existed inorganic ions, non-toxic natural organic matter (NOM) and self-quenching. Therefore, more catalyst/oxidant and energy have to be input to degrade the target pollutants. Fortunately, the selective oxidation of the target contaminants could address the above problems. Recent reports revealed that non-radicals like singlet oxygen ($^1O_2$), high-valent metals (HVMs) were generated to dominate the oxidation process, which exhibited selective decontamination and was slightly inhibited by the co-existed inorganic ions or NOM [11–13]. Moreover, selective oxidation could be achieved based on the differences of the contaminants in electron-donating/withdrawing properties,

---

ionization potential, molecule size, and so on [14–16]. It is believed that the development of selective oxidation is of greatly significant in water treatment.

The strategies for selective oxidation in both homogeneous and heterogeneous systems had been well summarized by Pan's group in very recently [17]. However, the selective oxidation over metal–organic frameworks (MOFs) catalysts was not highlighted up to now. MOFs are inorganic–organic hybrid materials built up by various metal ions/clusters and different organic ligands, which possess adjustable pore structure, large specific surface area and uniform metal active sites [18,19]. These unique physical and chemical properties make MOFs charming in various fields like adsorption, separation, catalysis, gas storage, drug delivery, sensing and so on [20–30]. Nowadays, MOFs and their composites/derivatives as (photo)catalysts for wastewater treatment have become a hotspot. There are many reviews on MOFs and their composites/derivatives for water treatment via AOPs, including photocatalysis [31–34], persulfate activation [35–40], Fenton-like [41–44] and so on [45,46]. These reviews have summarized the strategies to enhance the catalytic performance by MOFs-based catalysts (including pristine MOFs, membranes/films, composites, derivatives and so on), as well as the influence factors on degradation. It was deemed that MOFs have bright future in water purification. Moreover, our recent report demonstrated that MOFs-based catalysts could be continuously applied for decontaminant via persulfate activation [47], further confirming their huge potential in practical wastewater treatment. In addition, MOFs with different sizes and morphologies can be controllably prepared by various methods like hydro/solvothermal [48], microwave assisted method [49], sonochemical method [50], mechanochemical method [51], electrochemical method [52] and so on [53–55]. Based on their unique advantages and large application potential in water treatment, we believed that MOFs would bring new opportunity in selective oxidation. However, up to now, a few reports focus on selective oxidation over MOFs-based materials. Consequently, it is significant to summary the current research progress and propose the development direction in the near future.

In this review, the selective oxidation strategies over MOFs and their composites/derivatives for water treatment are summarized. Some examples are discussed in detail to show how MOFs-based materials realize selective oxidation. Finally, the outlook of selective oxidation over MOFs-based materials in aqueous is proposed.

2. The current state of selective oxidation by MOFs-based catalysts

The research progress of selective oxidation by MOFs-based catalysts was listed in Table 1, in which their applications and the origin of selective oxidation were highlighted. Further, the strategies for selective decontamination were interpreted in detail, and their corresponding influence factors were discussed.

From Table 1, it can be seen that the selective oxidation could be achieved by the in-situ generated reactive species, as well as controlling the contact between the reactants (Fig. 1). There are four mainstream pathways for decontamination via AOPs: radical pathway, singlet oxygenation, HVMs and direct electron transfer. In photocatalysis, Fenton-like and electrocatalysis systems, the degradation processes are usually dominated by radical species, especially •OH and $O_2^{\cdot-}$. While in persulfate (PS, including peroxymonosulfate (PMS) and peroxydisulfate (PDS)) activation system, both radical and non-radical pathways could accomplish the oxidation. In comparison, non-radical pathways (like $^1O_2$, and HVMs) display higher selectivity, which prefer to decompose electron-rich contaminants/groups. Therefore, it was feasible strategy to boost the generation of non-radicals rather than radicals during AOPs to realize selective oxidation.

It was also an efficient approach for selective oxidation to control the contact between the target pollutants and the MOFs-based catalysts. The pollutants must contact the reactive sites/ROSs before being oxidized, whereas the half-life of the ROSs is generally short (ns ~ μs). Based on the difference of the pollutants or pollutants and the water constituents like NOM in molecules size, ionization potential, hydrophobicity and so on, selective oxidation could be achieved by preparing suitable MOFs based membranes and/or composites/derivatives.

2.1. Selective oxidation induced by $^1O_2$

The non-radical $^1O_2$ is an excited state of O_2 with a short lifetime (3 μs) in H_2O [67]. It was known that the lifetime of $^1O_2$ can be extended to 68 μs in D_2O [68]. The $^1O_2$ possesses high selectivity, which prefers to attack nucleophiles. Therefore, it is prone to oxidize organic pollutants with electron donating functional groups like –OH, –NH$_2$ and alkyl group. In AOPs over MOFs-based materials, $^1O_2$ is one of common ROSs for decontaminant. For instance, in our recent studies, $^1O_2$ was generated in Co-MOF/PMS system [69], Co-MOF derived CoS_x/PMS system

Table 1
Selective oxidation of MOFs-based catalysts.

Catalyst	Organic pollutant/Removal efficiency (%)	Co-existing substance/Removal efficiency (%)	Oxidant/ irrigation	Dominant mechanism	Ref
FeCo MOF	CR/95 %, RhB/99 %, MO/95 %, BPA/100 %	3-NP/40 %, p-BA /50 %	PMS	$^1O_2$	[56]
Fe-MOF membrane	BPS/75.7 %	BA/-	H_2O_2	Size exclusion	[57]
MIL-53(Fe)@ anionic resin	MB/84 %	SRB/11 %	visible light	Electrostatic interaction	[58]
MIL-53(Fe)@ cationic resin	SRB/73 %	MB/59 %	visible light	Electrostatic interaction	[58]
Fe-BTC@resin	MB/71 %	SRB/12 %	visible light	Electrostatic interaction	[59]
Fe-MOF@MIP	SMX/97 %	BA/-	PS	MIT	[60]
Fe-MOF-74@MIP	DMP/95 %	DEP/80 %, DBP/70 %, DEHP/70 %	PS	MIT	[61]
Fe-MOF-74@SiO$_2$@MIP	DMP/93 %	DEP/68 %, OG/18 %, SMX/23 %	PS	MIT	[62]
Zn$_4$Co$_1$ − C	Phenol/100 %	BA/1%	PMS	$^1O_2$	[63]
yolk-shell Co/C	BPA/100 %	BA/-	PMS	Size exclusion	[64]
Cu/RGO	2,4-DCP/95.8 %	BA/0%, CBZ/10 %, IBU/30 %	PDS	Cu(III)	[65]
Fe/Fe$_3$O$_4$@rGO	BPA/90 %, BPF/60 %, MeP/12 %, p-BA/13 %, 2,4-DCP/100 %, CP/30 %, BPS/12 %, phenol/12 %	–	PDS	Hydrophobicity	[66]

Note: BTC = 1,3,5-tricarboxylic acid; MIP = molecular imprinted polymer; RGO = reduced graphene oxide; MIT = molecularly imprinted technology; CR = congo red; RhB = rhodamine B; MO = methyl orange; BPA = bisphenol A; BPS = bisphenol S; SRB = sulphorhodamine B; MG = malachite green; CV = crystal violet; MB = methylene blue; R6G = rhodamine 6G; SMX = sulfamethoxazole; DMP = dimethyl phthalate; 2,4-DCP = 2,4-dichlorophenol; BPF = bisphenol F; MeP = methyl-paraben; *p*-BA = 4-hydroxybenzaldehyde; CP = 4-chlorophenol; 3-NP = 3-nitrophenol; BA = benzoic acid; CBZ = carbamazepine; IBU = ibuprofen.
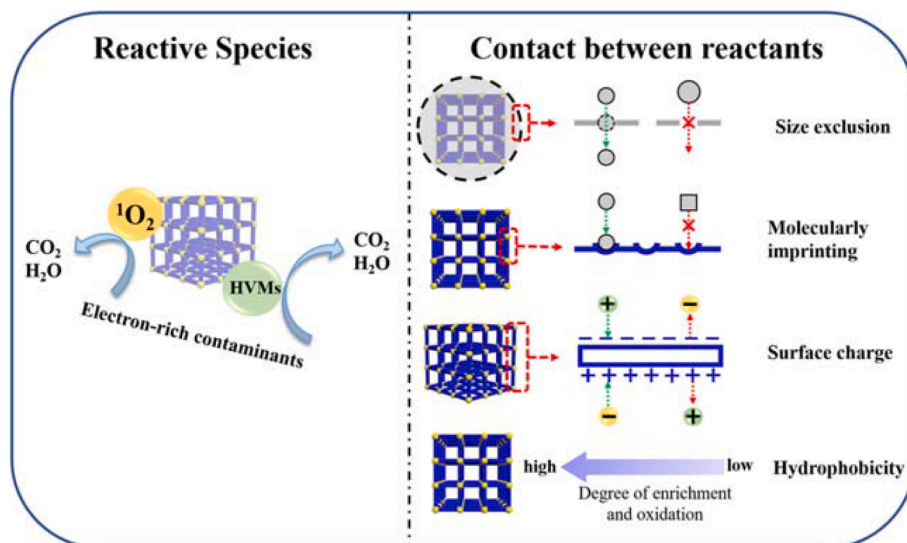
Fig. 1. Overview of the strategies for selective degradation of organic pollutants by MOFs-based catalysts.

[70], Fe-MOF composite/PDS system [71], Fe-MOF derived Fe_3O_4/PDS system [72], Fe-MOF derived Fe_3S_4/H_2O_2 system [73] and so on [74–76]. But other ROSs such as SO_4^-, •OH and O_2^- were also generated to contribute the oxidation process, leading to low selectivity.

In the PMS activation system with FeCo bimetallic MOF nanosheet (denoted as FeCo-BDC, BDC = 1,4-dicarboxybenzene) as catalyst, selective oxidation of organic pollutants was observed although both non-radical $^1O_2$ and radicals were generated [56]. Electron-rich organic dyes (such as RhB, CR, MO) and persistent organics (like BPA) were efficiently degraded in FeCo-BDC/PMS systems (Fig. 2a and b), whose mechanisms were illustrated in Fig. 2c. In the system, both dissolved oxygen and PMS could yield O_2^- (Eqs. (1) and (2)), which can be further converted to $^1O_2$ (Eqs. (3) and (4)) [77]. In addition, persulfate radicals (SO_5^-) can generate $^1O_2$ via self-reaction process (Eqs. (5) and (6)) [78]. The formed $^1O_2$ finally degraded electron-rich contaminants. During the reaction, Co^{3+} was reduced by HSO_5^- to Co^{2+} due to the higher redox potential of Co^{3+}/Co^{2+} (1.84 V) than that of HSO_5^-/SO_5^- (1.10 V), resulting in the increase of Co^{2+}/Co^{3+} ratio. Similar result was found in

monometallic Co-MOF/PMS system [69]. It is noted that some substances like 3-NP with electron withdrawing groups was also oxidized partially (Fig. 2b), in which the radicals like SO_4^- and •OH were also generated in the FeCo-BDC/PMS system.

$$O_2 + e^- \rightarrow O_2^- \tag{1}$$

$$SO_5^{2-} + H_2O \rightarrow SO_4^{2-} + •O_2^- + 2H^+ \tag{2}$$

$$O_2^- + O_2^- + 2H^+ \rightarrow {}^1O_2 + H_2O_2 \tag{3}$$

$$O_2^- + •OH \rightarrow {}^1O_2 + OH^- \tag{4}$$

$$HSO_5^- \rightarrow SO_5^- + H^+ + e^- \tag{5}$$

$$SO_5^- + SO_5^- \rightarrow {}^1O_2 + 2SO_4^{2-} \tag{6}$$

To enhance selective degradation efficiency, many efforts have been devoted to yield most $^1O_2$ and minimum generation of radical. For instance, Mi et al demonstrated almost 100 % conversion from PMS to
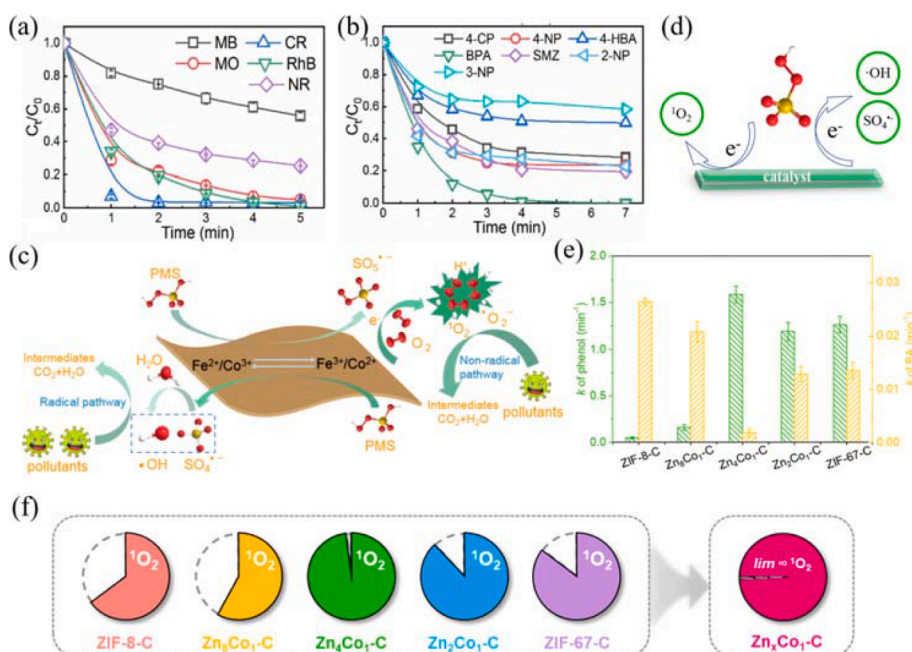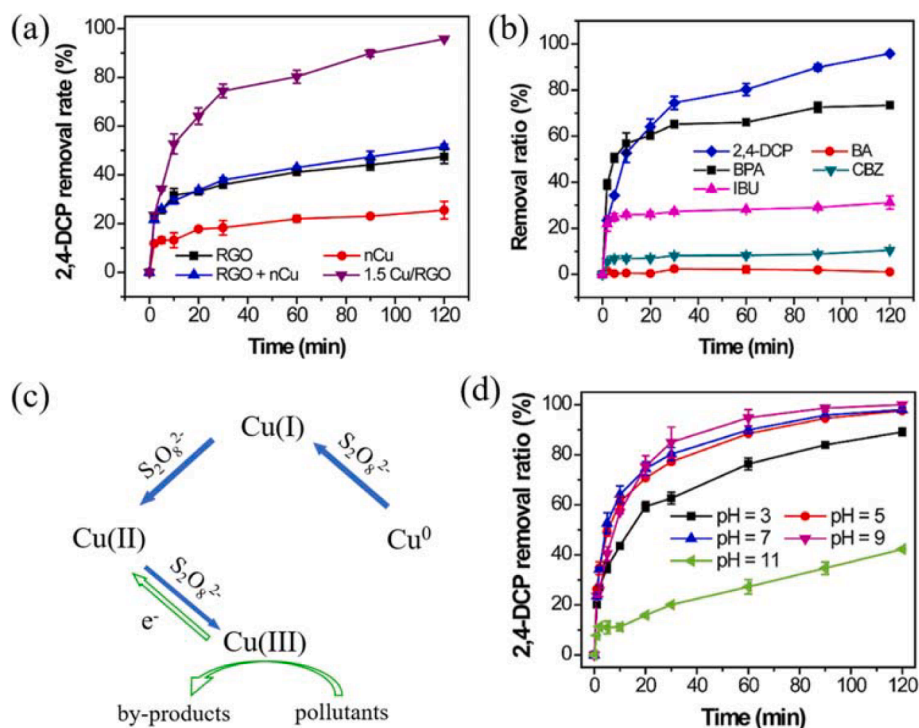

Fig. 2. (a and b) Selective oxidation of organic pollutants in FeCo-BDC/PMS systems. (c) Degradation mechanism of contaminations in FeCo-BDC/PMS system. Reproduced with permission from Ref. [56]. (d) The relationship between the adsorbed sites of PMS and $^1O_2$ generation. (e) Reaction rate (k value) of Co—N—C catalysts in oxidation of phenol/BA solution. (f) Effects of Zn/Co ratio in the precursor on $^1O_2$ yield in PMS activation system. Reproduced with permission from Ref. [63].

$^1O_2$ over a Co—N—C catalyst derived from Zn/Co bimetallic MOF [79]. The single Co atom sites were located by electronegative nitrogen atoms to form CoN_{2+2} sites. During PMS activation, one oxygen atom from $-SO_4$ of PMS was prone to be chemically adsorbed by the single Co atom, which could donate electrons to Co sites. The Co atom was reduced while the adsorbed PMS was oxidized and generated $^1O_2$ finally (Eqs. (5) and (6)). Interestingly, •OH and $SO_4^{\cdot-}$ instead of $^1O_2$ were generated when single Co atom was replaced by Co nanoparticles (Co-NP) as catalyst. This was because that PMS would be molecularly adsorbed by the positively charged Co-NP, where the strong interaction between Co and oxygen atoms from PMS would lead to spontaneous dissociation of the PMS molecule to form •OH and $SO_4^{\cdot-}$ radicals (Fig. 2d) [79]. In order to further unravel the relationship between Co—N—C structure and the yield of $^1O_2$, Yao et al. regulated Co—N—C coordination by annealing bimetallic Zn/Co-ZIFs with different Zn/Co ratio [63]. The Zn/Co ratios in the precursor were set as 8:1, 4:1 and 2:1, and the corresponding derivatives were demoted as Zn8Co1-C, Zn4Co1-C and Zn2Co1-C, respectively. It was found that higher Co content would result in lower N content. Consequently, Co nanoparticles rather than Co-N tended to be formed in Zn2Co1-C. When the Co content was extremely low (like Zn8Co1-C), Zn and Co would co-coordinate with N atoms. In comparison, single Co atom coordinated with four N atoms to form abundant CoN_4 sites in Zn4Co1-C. Among Zn8Co1-C, Zn4Co1-C, Zn2Co1-C and monometallic ZIF-8/ZIF-67 derivatives (ZIF-8-C and ZIF-67-C, respectively), Zn4Co1-C exhibited the highest $^1O_2$ yield (Fig. 2f). The selectivity of the Co—N—C catalysts were tested by a mixed solution containing phenol and benzoic acid (BA). Phenol can be degraded by both radicals (like •OH, $SO_4^{\cdot-}$) and non-radicals (like $^1O_2$), whereas BA can only be oxidized by radicals [80]. As showed in Fig. 2e, the fastest phenol removal efficiency along with the slowest BA degradation occurred in the Zn4Co1-C/PMS system, further confirming the maximum $^1O_2$ yield over Zn4Co1-C.

2.2. Selective oxidation induced by HVMs

In AOPs, the generated ROSs are usually consumed by the co-existing constituents such as inorganic anions, leading to low oxidant utilization [81]. It was reported that HVMs like Cu(III), Fe(IV) and Co(IV) could be formed in AOP systems, which not only showed strong oxidative ability regardless of the co-existing constituents, but also have high selectivity towards electron-donating groups [82–84]. These advantages are comparable with that of $^1O_2$. Differently, HVMs species can be formed with consumption of equimolar PMS, while double PMS is needed to generate one molar $^1O_2$ [12]. Consequently, oxidation processes induced by HVMs display higher PS utilization than that by radicals or $^1O_2$. But the influence of solution pH on the metals form shouldn't be ignored, because it would change the reduction potential of the metals. For instance, the reduction potential of Cu(III)/Cu(II) in solid phase is 2.3 eV, while it decreases to 1.57 eV in ionized form [85].

Liu et al. reported selective degradation induced by Cu(III) species over Cu/RGO derived from Cu-MOF@RGO composite [65]. The sizes of Cu nanoparticles in the catalyst (denoted as 1.5 Cu/RGO) was 80 ~ 100 nm. As showed in Fig. 3a, 1.5 Cu/RGO exhibited superior 2,4-DCP oxidation performance over nano Cu^0 (nCu), RGO and nCu/RGO under the identical conditions. However, some selected aromatic compounds like BA and CBZ were slightly oxidized (Fig. 3b). This was because that the electron-withdrawing groups was hard to be oxidized by HVMs. The generation pathway of Cu(III) was displayed in Fig. 3c. It was demonstrated that Cu^0 reacted with PDS to produce Cu(I), Cu(II) and Cu(III) gradually. As displayed in Fig. 3d, the target contaminant was efficiently degraded in a wide range of pH values (3 ~ 9). But the form of Cu in the acid and the basic conditions is deserved to be noted. In acid condition (pH = 3), partial solid Cu(III) might leach into the solution to form Cu^{3+} ion. The degradation of 2,4-DCP was seriously inhibited when pH value was 11, since that $Cu(OH)^{2+}$ and $Cu(OH)_2^+$ were formed to occupy the surface of the Cu nanoparticles [65].

Fig. 3. (a) Degradation efficiencies of 2,4-DCP in PDS activation systems over different catalysts. (b) Degradation efficiencies of 2,4-DCP, BA, BPA, CBZ and IBU in 1.5 Cu/RGO/PDS systems. (c) Degradation mechanism of contaminations in 1.5 Cu/RGO/PDS system. (d) Influence of initial pH on degradation of 2,4-DCP by 1.5 Cu/RGO. Reproduced with permission from Ref. [65].

2.3. Selective oxidation induced by size exclusion

In actual water treatment via AOPs, the generated ROSs are usually consumed by macromolecular components like NOM, resulting in decrease of degradation efficiency. The co-existed NOM are much larger than organic pollutants such as tetracycline antibiotics, perfluorochemicals and phenols in size. Consequently, they can be intercepted based on size before oxidation process. Yolk-shell (or core–shell) structure, encapsulating catalysts by a porous shell with specific size, is an ideal strategy to exclude co-existed large molecules. When the shell is much larger than the core, the confinement effect may be formed and significantly promote the reaction kinetics [86]. Yolk-shell structure with cavity between the catalyst (core) and shell is promising not only in selective removal of multi-component contaminants [87], but also in enriching trace contaminants from aqueous system.

Zhang et. al prepared a yolk-shell nanoreactor derived from ZIF-67 for oxidation of organic pollutants [64]. As showed in Fig. 4a, BPA was completely degraded within 15 min over yolk-shell nanoreactor (denoted as YSCCNs). In presence of 10 mM humic acid (HA), the BPA degradation was hardly inhibited. This was because that BPA (1.07 nm) and PMS could get through the shell pore channel (1.5 ~ 3.0 nm) and contact the internal active sites (Co/C nanoparticles), whereas the macromolecule HA was excluded by the shell (Fig. 4b). When the HA concentration increased to 20 mM, BPA removal rate slightly decreased from 0.41 min^{-1} to 0.22 min^{-1}, which contributed to the blocking of shell channels and the occupation of the surficial active sites by the high concentration HA. Besides core–shell structured catalysts, MOFs-based micro/nanoreactors with different morphologies deserve more exploration, since the morphology could greatly influence the reaction process. For instance, Fe_2O_3 was loaded in carbon nanotube for decontamination via electro-Fenton reaction, which not only realize selective oxidation, but also accelerated mass transfer [88].

Another feasible strategy for macromolecular components removal is embedding MOFs-based catalysts into porous membranes/films covered by a skin layer with special pore/channel sizes. The skin layer of the bifunctional membranes/films would exclude macromolecular components, whereas the support layer containing MOFs-based catalysts possess good permeability and high catalytic activity (Fig. 4c). For instance, Ren et al. casted dual-layer membrane denoted as Seq-ICM for sequential interception of macromolecular components and oxidation via Fenton-like reaction [57]. The skin layer was dense enough to intercept macromolecular substances such as HA, bovine serum albumin and dextran. As illustrated in Fig. 4d, 65.3 % of total organic carbon (TOC) in solution containing 4,4′-sulphonyl diphenol (BPS) and bovine serum albumin (BSA) was removed, while only 1.9 % of BPS was oxidized. The decrease of TOC was contributed to the interception of BSA rather than degradation. The adsorption of BSA over the support layer containing ca. 50 % MIL-53(Fe) was negligible (4.1 %), but 39.4 % TOC could be removed via Fenton-like reaction. In comparison, both fast BSA interception and efficient BPS degradation could achieve in Seq-ICM system with addition of H_2O_2, which was much better than that of the simple combination of skin layer and support layer (denoted as Sim-ICM).

Size exclusion is of great significant in practical selective oxidation, since it can reduce the consumption of ROSs by the low-toxic compounds in the water like NOM. Consequently, the generated ROSs can fully oxidize high-toxicity organic pollutants to low-toxic ones even mineralize them to CO_2. Nevertheless, it is still expected to develop a strategy to anchor and decompose the special functional groups, which might be more efficient for detoxification. In addition, the regeneration of the nano-reactor and the bi-functional membranes/films should be further studied to reduce their cost.

2.4. Selective oxidation induced by molecularly imprinted technology

Molecularly imprinted technology (MIT) has been applied in many files like solid-phase extraction, chemical sensing, catalysis, and drug delivery due to its robust molecular recognition ability, low cost, easy preparation and high stability [89,90]. This strategy can evaluate the selectivity of MOFs-based materials by creating tailor-made sites with special shape and size of the target contaminants, as illustrated in Fig. 5a. The target pollutants would be specifically adsorbed and degraded, while the co-existing matters would be excluded away from active sites. For instance, SMX was efficiently enriched and degraded in
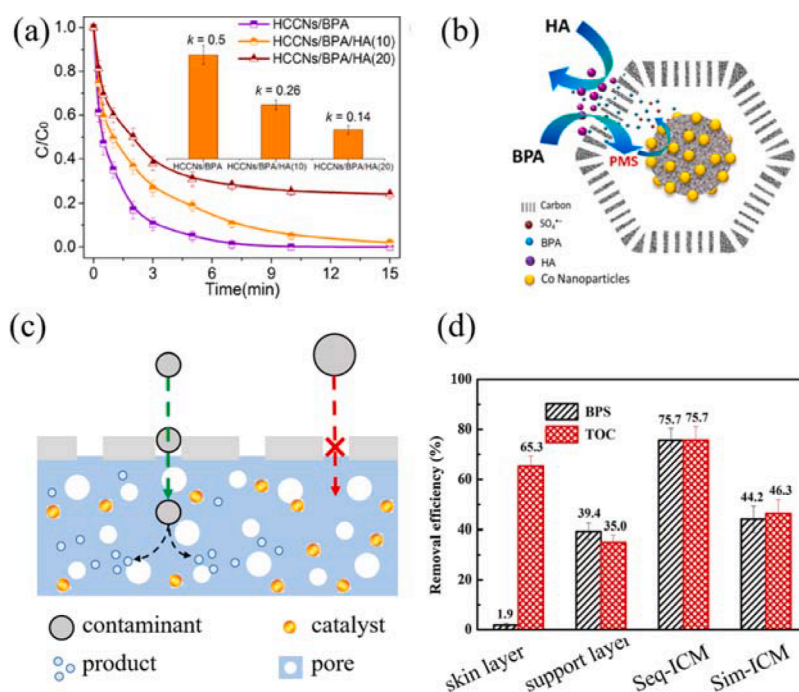
Fig. 4. (a) BPA degradation over YSCCNs in absence/presence of HA. (b) The size exclusion over YSCCNs. Reproduced with permission from Ref. [64]. (c) dual-layer membrane for selective oxidation. (d) BPS and TOC removal in skin layer, support layer, Seq-ICM and Sim-ICM systems. Reproduced with permission from Ref. [57].
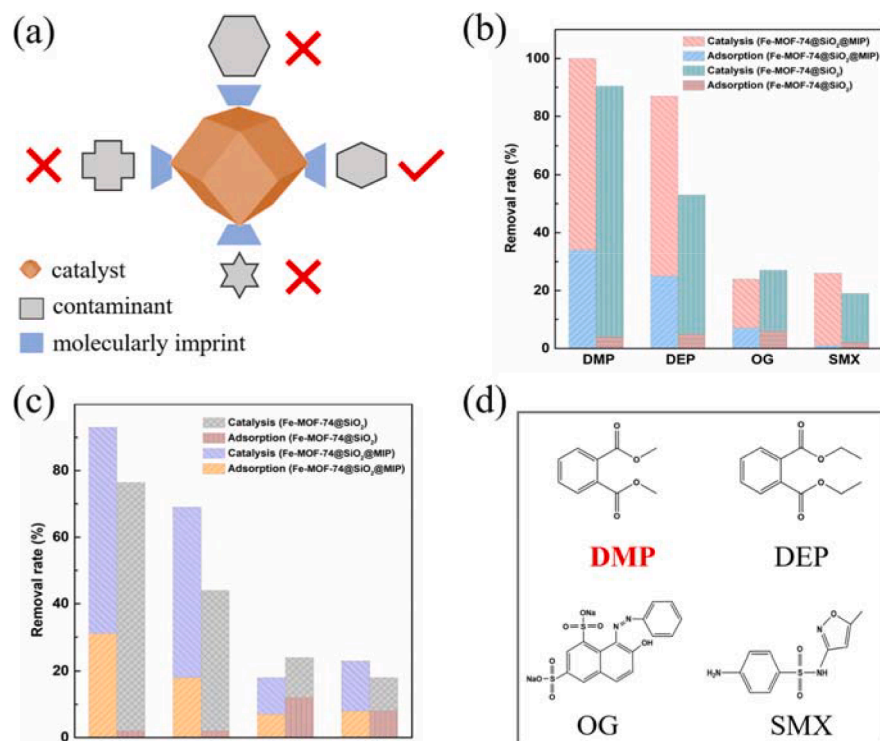
Fig. 5. (a) Molecularly imprinted technology for selective oxidation. (b) Removal of DMP, DEP, OG and SMX from sole solution. (c) Selective removal of DMP, DEP, OG and SMX in mixed solution. Reproduced with permission from Ref. [62]. (d) Structure schemes of DMP, DEP, OG and SMX.

molecularly imprinted channels from a Fe-MOF catalyst by specific recognition sites, whereas the co-exiting ciprofloxacin and tetracycline were hardly adsorbed or decomposed [60]. But when the co-existing substances have similar functional groups to those of the target contaminant, the competed adsorption and degradation would occur. As showed in Fig. 5b, the target organic pollutant DMP was completely removed by Fe-MOF-74@SiO$_2$@MIP from individual DMP solution via PS activation. OG and SMX were excluded by the MIP, resulting in low removal efficiency. However, DEP could be adsorbed and decomposed efficiently due to the existence of ester group and benzene ring (Fig. 5d). When DMP was mixed with DEP, OG and SMX, no obvious decline of OG or SMX removal could be found. In comparison, the removal efficiencies of both DMP and DEP were decreased due to the competitive interaction between DMP and DEP (Fig. 5c) [62].

As displayed in Fig. 5a, the induced molecularly imprint increase adsorption sites and accelerate the enrichment of the target pollutants on the catalysts surface. However, it would separate the targets from the active sites as well [91,92]. Consequently, the oxidation efficiency toward the target contaminants mainly depends on the ROSs. In addition, the influences of pH value and co-existing ions/anions on the selectivity of MIP should be noted.

2.5. Selective oxidation induced by surface charge

The surface charge of catalysts is mainly determined by their functional groups [17]. Generally, pollutants with counter charge to catalysts would be preferentially adsorbed/enriched and then oxidized. On the contrary, the target pollutants molecules with the same charge would be repulsed from the surface of catalysts, resulting in low removal efficiency. For MOFs, they can be easily modified with diverse functional groups, but few selective oxidation examples by this strategy are reported to date. This maybe because that the electrostatic interaction between the organic pollutants and catalysts is greatly influenced by solution pH, and the adsorption/enrichment process would be co-determined by π–π interaction, hydrogen bonding and so on [93]. In

order to strengthen the electrostatic interaction between MOFs and organic pollutants, some anionic/cationic materials were used to prepare composites with MOFs-based catalysts (Fig. 6a). For instance, MIL-53(Fe) was composited with anionic resins (denoted as AMIL-53(Fe)) and cationic resins (denoted as DMIL-53(Fe)) for selective removal of cationic dyes and anionic dyes, respectively [58]. The abundant sulfonyl groups in the anionic resin endows the AMIL-53(Fe) with strong acidity, along with zeta potential of −24 mV at the optimal ratio (20 %) of anionic resin to MIL-53(Fe). For DMIL-53(Fe), the quaternary ammonium groups in the cationic resin makes it strong alkalinity, and the zeta potential was +2 mV at the identical ratio of cationic resin. During photocatalysis reaction, the cationic RhB was preferentially adsorbed by AMIL-53(Fe) and being degraded efficiently, which was much better than that of anionic SRB. However, the contrary results could be observed over DMIL-53(Fe) (Fig. 6b), although the active species (photogenerated holes and O$_2^-$) were the same in both AMIL-53(Fe) and DMIL-53(Fe) systems (Fig. 6c).

2.6. Selective oxidation induced by hydrophobicity

Hydrophobicity and hydrophilicity of contaminants exerted great influence on oxidation process in heterogenous catalysis system, which can affect the surface enrichment of organic pollutants on the catalysts [94,95]. For hydrophobic organic pollutants, they might be enriched near the surface of the hydrophobic catalysts, which is beneficial for their preferential degradation. In a study of phenolic compounds degradation over graphene oxide@Fe-MOF derivative (denoted as rGOF), Liu et al. found that the degradation kinetic rate depended on the hydrophobicity of the compounds [66]. The hydrophobicity of the targets was BPA > 2,4-DCP > BPF > CP > MeP > BPS > p-BA > phenol (PE). As illustrated in Fig. 7a and b, compounds with larger XLog *P* value, meaning stronger hydrophobicity, exhibited larger adsorption capacity in single contaminant solution. The enriched contaminants were decomposed by the generated ROSs like $^1O_2$, •OH and SO_4^-, in which the degradation rates (k_1) displayed the positive correlation with
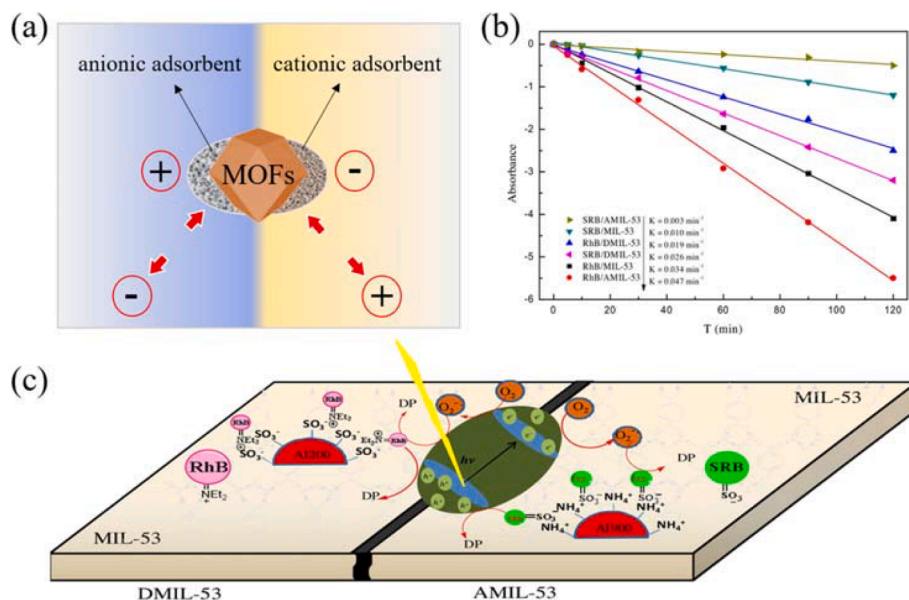
Fig. 6. (a) Electrostatic interaction between MOFs-based catalysts and cationic/anionic contaminants. (b) Photocatalytic degradation of RhB, SRB and their (c) mechanisms on MIL-53(Fe), AMIL-53(Fe) and DMIL-53(Fe). Reproduced with permission from Ref. [58].
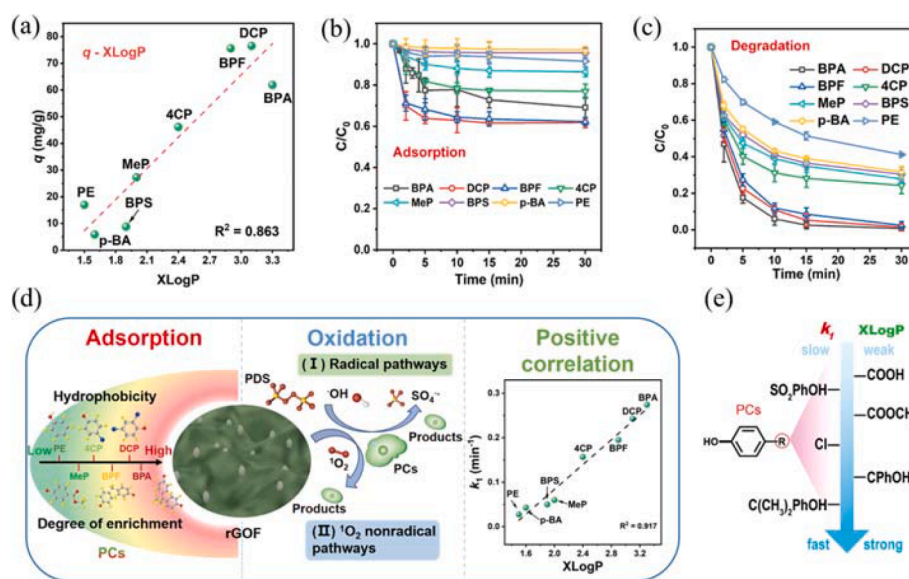
Fig. 7. (a) Correlation of adsorption capacity (q) and XLog P value. (b) Adsorption of phenolic compounds over rGOF. (c) Degradation of phenolic compounds in rGOF/PDS system. (d) Selective phenolic compounds removal in rGOF/PDS system. (e) Relationships between reaction rate (k_1), XLog P value and the functional groups in phenolic compounds. Reproduced with permission from Ref. [66].

the hydrophobicity of the compounds (Fig. 7c and d). In detail, the removal rate (k_1) of the phenolic compounds in the rGOF/PDS system relied on their hydrophobicity, which was determined by the groups in the phenolic ring. As shown in Fig. 7e, the functional group with larger XLog P value possessed stronger hydrophobicity, leading to faster removal rate. However, the enrichment process of the target contaminant might be affected by the co-existing substances. For instance, the removal rate of BPA was faster than that of DCP in single solution, while it exhibited opposite results in the mixture. This was because the electron-donating groups (Cl$^-$) in the DCP were more prone to be oxidized, especially by $^1O_2$ in the competitive environment [66,96].

3. Further discussion on the potential of MOFs in selective oxidation

The pristine MOFs and their composites/derivatives can achieve selective oxidation for wastewater treatment. For pristine MOFs, various structures can be obtained via changing organic linkers and/or metal ions. To date, more than 20,000 MOFs are designed and synthesized [97]. It is feasible to modify/graft some special functional groups to strengthen MOFs' target performance. For instance, Yang et al. decorated MIL-101 by -SO$_3$H on the ligands to enhance anionic dyes adsorption [98]. Besides, the defect engineering is also an efficient strategy to enhance MOFs' performance [99].

MOFs composites usually exhibit better performance than the pristine ones in catalysis and separation due to the synergetic effect between MOFs and the functional materials. These functional materials include

but not limit to MOFs [100], g-C$_3$N$_4$ [101], graphene oxide [102], metallic oxide [103] and metal sulphide [104]. Composites can be simply fabricated by both in situ growth and post synthetic methods, in which MOFs can maintain their structures and original morphologies. Therefore, it is feasible to change properties of MOFs-based materials by preparing composites (such as MIP and core–shell structures) to realize the selective oxidation.

Compared to pristine MOFs, their derivatives like metal/carbon hybrids might be more environmentally friendly and more stable in liquid. Moreover, these metal/carbon hybrids usually maintain unique advantages of MOFs, including but not limit to: (1) highly dispersed metal nanoparticles or single metal atom rather than bulk metal particles, due to the uniform metal nodes in MOFs; (2) large specific surface area; (3) diverse morphologies by tailoring MOFs morphologies or changing derivatization conditions; (4) hierarchical pores structures, enhancing the utilization of the internal active sites; (5) multi-elements such as N, O, S, Co and Fe dispersedly in the derivatives by selecting suitable MOFs as precursors. These advantages endow MOFs derivatives with huge potential in selective oxidation.

Moreover, with the continuous development of synthetic methods, MOFs with various morphologies (such as monodisperse particles, nanowires, nanosheet, hollow MOFs) and different sizes could be obtained. These manipulations could further optimize the physical properties of MOFs-based materials including individual MOFs, composites/derivatives as well as membranes/films. In all, it broadens the application scenario of MOFs-based catalysts for selective oxidation in water treatment.

4. Conclusions and prospective

Emerging research has demonstrated MOFs-based catalysts to be candidate for selective oxidation in wastewater treatment. The pristine MOFs as well as their composites/derivatives can realize selective oxidation base on two pathways: reactive species ($^1O_2$ and high-valent metals) and selective contact (including size exclusion, molecularly imprinted technology, surface charge, hydrophobicity) between catalysts and contaminants. Considering the complicated compositions in wastewater, it might be promising to combine diverse pathways for selective oxidation in actual wastewater treatment.

Although MOFs-based materials are demonstrating large potential in selective oxidation for wastewater treatment, there are still some key issues to be concerned. (1) Low-cost and high throughput production of MOFs-based materials are expected. Many technologies like electrochemical method, mechanochemical method are considered to efficiently synthesize MOFs, but only a few MOFs can achieve pilot-scale production to date [105]. On the other hand, calcination and pyrolysis are the main methods to prepare MOFs derivatives, which is energy consuming [106]. Therefore, it is necessary to develop green strategies to fabricate MOFs-based materials. (2) Some single metal atom (Co for instance) catalysts derived from MOFs were designed to promote $^1O_2$ generation in PMS activation system, but it still remains challenge to tune the formation of high valent metals or $^1O_2$ in other AOPs systems. (3) The oxidation mechanism of organic pollutants should be further explored. The radicals and non-radicals are usually detected in AOPs systems, but the formation and the roles of these reactive species are still unclear. Additionally, the reaction conditions like light irradiation, pH, co-existing matter, oxidant concentration might affect the reaction mechanism and the selectivity. It was necessary to combine advanced characterization and theoretical calculation to clarify the degradation mechanism in different AOPs systems. (4) Researchers mainly focus on PS activation systems for selective oxidation, but the environmental risk from the continuous input of sulfate should be concerned. (5) Size exclusion is a charming pathway for selective oxidation, which is a spontaneous process without extra energy input. Various structures like MOF-on-MOF should be developed to further study the potential application of size exclusion. (6) Many MOFs-based catalysts like yolk-

shell reactor were prepared as powder or micro/nano particles, which was difficult to accomplish recovery and recycle. Therefore, immobilizing MOFs-based catalysts on some suitable substrates or fabricating MOF-based membranes are great of significant for selective oxidation in actual wastewater treatment. In all, it is expected that MOFs-based functional materials would be widely developed for selective oxidation toward emerging pollutants in wastewater treatment.

Declaration of Competing Interest

The authors declare that they have no known competing financial interests or personal relationships that could have appeared to influence the work reported in this paper.

Data availability

No data was used for the research described in the article.

Acknowledgements

References

[1] C.I. Ezugwu, J.M. Sonawane, R. Rosal, Redox-active metal-organic frameworks for the removal of contaminants of emerging concern, Sep. Purif. Technol. 284 (2022), 120246.

[2] F.T. Alshorifi, S.L. Ali, R.S. Salama, Promotional Synergistic Effect of Cs–Au NPs on the Performance of Cs–Au/MgFe2O4 Catalysts in Catalysis 3,4-Dihydropyrimidin-2(1H)-Ones and Degradation of RhB Dye, J. Inorg. Organomet. Polym Mater. 32 (2022) 3765–3776.

[3] V. Kavitha, Global prevalence and visible light mediated photodegradation of pharmaceuticals and personal care products (PPCPs)-a review, Results Eng. 14 (2022), 100469.

[4] J. Wang, S. Wang, Activation of persulfate (PS) and peroxymonosulfate (PMS) and application for the degradation of emerging contaminants, Chem. Eng. J. 334 (2018) 1502–1517.

[5] X. Hu, J. Bao, D. Chen, S. Jalil Shah, S. Subhan, W. Gong, W. Li, X. Luan, Z. Zhao, Z. Zhao, Accelerating the Fe(III)/Fe(II) cycle via enhanced electronic effect in NH2-MIL-88B(Fe)/TPB-DMTP-COF composite for boosting photo-Fenton degradation of sulfamerazine, J. Colloid Interface Sci. 624 (2022) 121–136.

[6] F.-X. Wang, C.-C. Wang, X. Du, Y. Li, F. Wang, P. Wang, Efficient removal of emerging organic contaminants via photo-Fenton process over micron-sized Fe-MOF sheet, Chem. Eng. J. 429 (2022), 132495.

[7] K. Wenderich, G. Mul, Methods, Mechanism, and Applications of Photodeposition in Photocatalysis: A Review, Chem. Rev. 116 (2016) 14587–14619.

[8] A. Babuponnusami, K. Muthukumar, A review on Fenton and improvements to the Fenton process for wastewater treatment, Journal of Environmental, Chem. Eng. 2 (2014) 557–572.

[9] X. Du, M.A. Oturan, M. Zhou, N. Belkessa, P. Su, J. Cai, C. Trellu, E. Mousset, Nanostructured electrodes for electrocatalytic advanced oxidation processes: From materials preparation to mechanisms understanding and wastewater treatment applications, Appl. Catal. B 296 (2021), 120332.

[10] U. von Gunten, Ozonation of drinking water: Part I. Oxidation kinetics and product formation, Water Res. 37 (2003) 1443–1467.

[11] J. Li, Y. Zhao, X. Wang, T. Tang, X. Hou, Rapid microwave synthesis of PCN-134-2D for singlet oxygen based-oxidative degradation of ranitidine under visible light: Mechanism and toxicity assessment, Chem. Eng. J. 443 (2022), 136424.

[12] Y. Wei, J. Miao, J. Ge, J. Lang, C. Yu, L. Zhang, P.J.J. Alvarez, M. Long, Ultrahigh Peroxymonosulfate Utilization Efficiency over CuO Nanosheets via Heterogeneous Cu(III) Formation and Preferential Electron Transfer during Degradation of Phenols, Environ. Sci. Technol. 56 (2022) 8984–8992.

[13] Y. Fu, K. Zhang, Y. Zhang, Y. Cong, Q. Wang, Fabrication of visible-light-active MR/NH2-MIL-125(Ti) homojunction with boosted photocatalytic performance, Chem. Eng. J. 412 (2021), 128722.

[14] Z.-H. Xie, C.-S. He, H.-Y. Zhou, L.-L. Li, Y. Liu, Y. Du, W. Liu, Y. Mu, B. Lai, Effects of Molecular Structure on Organic Contaminants' Degradation Efficiency and

Dominant ROS in the Advanced Oxidation Process with Multiple ROS, Environ. Sci. Technol. 56 (2022) 8784–8795.

[15] S. Zhu, X. Li, J. Kang, X. Duan, S. Wang, Persulfate Activation on Crystallographic Manganese Oxides: Mechanism of Singlet Oxygen Evolution for Nonradical Selective Degradation of Aqueous Contaminants, Environ. Sci. Technol. 53 (2019) 307–315.

[16] L. Chen, S. Wang, Z. Yang, J. Qian, B. Pan, Selective interfacial oxidation of organic pollutants in Fenton-like system mediated by Fe(III)-adsorbed carbon nanotubes, Appl Catal B 292 (2021), 120193.

[17] Z. Yang, J. Qian, C. Shan, H. Li, Y. Yin, B. Pan, Toward Selective Oxidation of Contaminants in Aqueous Systems, Environ. Sci. Technol. 55 (2021) 14494–14514.

[18] C.-C. Wang, J.-R. Li, X.-L. Lv, Y.-Q. Zhang, G. Guo, Photocatalytic organic pollutants degradation in metal–organic frameworks, Energy Environ. Sci. 7 (2014) 2831–2867.

[19] F.-X. Wang, C.-C. Wang, P. Wang, B.-C. Xing, Syntheses and applications of UiO series of MOFs, Chin. J. Inorg. Chem. 33 (2017) 713–737.

[20] M. Li, J. Chen, W. Wu, Y. Fang, S. Dong, Oxidase-like MOF-818 Nanozyme with High Specificity for Catalysis of Catechol Oxidation, J. Am. Chem. Soc. 142 (2020) 15569–15574.

[21] J.P. Marco-Lozar, J. Juan-Juan, F. Suárez-García, D. Cazorla-Amorós, A. Linares-Solano, MOF-5 and activated carbons as adsorbents for gas storage, Int. J. Hydrogen Energy 37 (2012) 2370–2381.

[22] C.-Y. Wang, C.-C. Wang, X.-W. Zhang, X.-Y. Ren, B. Yu, P. Wang, Z.-X. Zhao, H. Fu, A new Eu-MOF for ratiometrically fluorescent detection toward quinolone antibiotics and selective detection toward tetracycline antibiotics, Chin. Chem. Lett. 33 (2022) 1353–1357.

[23] K. Suresh, A.J. Matzger, Enhanced Drug Delivery by Dissolution of Amorphous Drug Encapsulated in a Water Unstable Metal-Organic Framework (MOF), Angew. Chem. Int. Ed. 58 (2019) 16790–16794.

[24] J. Ma, C.-C. Wang, Z.-X. Zhao, P. Wang, J.-J. Li, F.-X. Wang, Adsorptive capture of perrhenate (ReO4−) from simulated wastewater by cationic 2D-MOF BUC-17, Polyhedron 202 (2021), 115218.

[25] Y. Wang, H. Jin, Q. Ma, K. Mo, H. Mao, A. Feldhoff, X. Cao, Y. Li, F. Pan, Z. Jiang, A MOF Glass Membrane for Gas Separation, Angew. Chem. Int. Ed. 59 (2020) 4365–4369.

[26] C.-Y. Wang, L. Ma, C.-C. Wang, P. Wang, L. Gutierrez, W. Zheng, Light-response adsorption and desorption behaviors of metal–organic frameworks, Environ. Funct. Mater. 1 (2022) 49–66.

[27] H. Fu, C.-C. Wang, W. Liu, MOFs for water purification, Chin. Chem. Lett. 33 (2022) 1647–1649.

[28] H.M. Altass, S.A. Ahmed, R.S. Salama, Z. Moussa, R.S. Jassas, R.I. Alsantali, M. M. Al-Rooqi, A.A. Ibrahim, M.A. Khder, M. Morad, A.I. Ahmed, A.S. Khder, Low Temperature CO Oxidation Over Highly Active Gold Nanoparticles Supported on Reduced Graphene Oxide@Mg-BTC Nanocomposite, Catal. Lett. (2022).

[29] S.A. Al-Thabaiti, M.M.M. Mostafa, A.I. Ahmed, R.S. Salama, Synthesis of copper/chromium metal organic frameworks - Derivatives as an advanced electrode material for high-performance supercapacitors, Ceram. Int. 49 (2023) 5119–5129.

[30] R.S. Salama, M.A. Mannaa, H.M. Altass, A.A. Ibrahim, A.-E.-R.-S. Khder, Palladium supported on mixed-metal–organic framework (Co–Mn-MOF-74) for efficient catalytic oxidation of CO, RSC Adv. 11 (2021) 4318–4326.

[31] S. Gautam, H. Agrawal, M. Thakur, A. Akbari, H. Sharda, R. Kaur, M. Amini, Metal oxides and metal organic frameworks for the photocatalytic degradation: A review, J. Environ. Chem. Eng. 8 (2020), 103726.

[32] T. Wu, X. Liu, Y. Liu, M. Cheng, Z. Liu, G. Zeng, B. Shao, Q. Liang, W. Zhang, Q. He, W. Zhang, Application of QD-MOF composites for photocatalysis: Energy production and environmental remediation, Coord. Chem. Rev. 403 (2020), 213097.

[33] V. Kumar, V. Singh, K.-H. Kim, E.E. Kwon, S.A. Younis, Metal-organic frameworks for photocatalytic detoxification of chromium and uranium in water, Coord. Chem. Rev. 447 (2021) 214148.

[34] C. Zhao, X. Pan, Z. Wang, C.-C. Wang, 1 + 1 > 2: A critical review of MOF/bismuth-based semiconductor composites for boosted photocatalysis, Chem. Eng. J. 417 (2021), 128022.

[35] C. Wang, J. Kim, V. Malgras, J. Na, J. Lin, J. You, M. Zhang, J. Li, Y. Yamauchi, Metal-Organic Frameworks and Their Derived Materials: Emerging Catalysts for a Sulfate Radicals-Based Advanced Oxidation Process in Water Purification, Small 15 (2019) 1900744.

[36] Z. Xiong, Y. Jiang, Z. Wu, G. Yao, B. Lai, Synthesis strategies and emerging mechanisms of metal-organic frameworks for sulfate radical-based advanced oxidation process: A review, Chem. Eng. J. 421 (2021) 127863.

[37] X. Du, M. Zhou, Strategies to enhance catalytic performance of metal–organic frameworks in sulfate radical-based advanced oxidation processes for organic pollutants removal, Chem. Eng. J. 403 (2021) 126346.

[38] M. Han, W. Zhu, M.S.A. Hossain, J. You, J. Kim, Recent progress of functional metal–organic framework materials for water treatment using sulfate radicals, Environ. Res. 211 (2022) 112956.

[39] D. Huang, G. Wang, M. Cheng, G. Zhang, S. Chen, Y. Liu, Z. Li, W. Xue, L. Lei, R. Xiao, Optimal preparation of catalytic Metal-organic framework derivatives and their efficient application in advanced oxidation processes, Chem. Eng. J. 421 (2021) 127817.

[40] X.-W. Zhang, M.-Y. Lan, F. Wang, X.-H. Yi, C.-C. Wang, ZIF-67-based catalysts in persulfate advanced oxidation processes (PS-AOPs) for water remediation, J. Environ. Chem. Eng. 10 (2022), 107997.

[41] X. Du, S. Wang, F. Ye, Z. Qingrui, Derivatives of metal-organic frameworks for heterogeneous Fenton-like processes: From preparation to performance and mechanisms in wastewater purification – A mini review, Environ. Res. 206 (2022), 112414.

[42] M. Cheng, C. Lai, Y. Liu, G. Zeng, D. Huang, C. Zhang, L. Qin, L. Hu, C. Zhou, W. Xiong, Metal-organic frameworks for highly efficient heterogeneous Fenton-like catalysis, Coord. Chem. Rev. 368 (2018) 80–92.

[43] C. Du, Y. Zhang, Z. Zhang, L. Zhou, G. Yu, X. Wen, T. Chi, G. Wang, Y. Su, F. Deng, Y. Lv, H. Zhu, Fe-based metal organic frameworks (Fe-MOFs) for organic pollutants removal via photo-Fenton: A review, Chem. Eng. J. 431 (2022), 133932.

[44] M.F. Dapaah, Q. Niu, Y.-Y. Yu, T. You, B. Liu, L. Cheng, Efficient persistent organic pollutant removal in water using MIL-metal–organic framework driven Fenton-like reactions: A critical review, Chem. Eng. J. 431 (2022), 134182.

[45] X.-H. Yi, C.-C. Wang, Elimination of emerging organic contaminations in wastewater by advanced oxidation process over iron-based MOFs and their composites, Prog. Chem. 33 (2021) 471–489.

[46] V.K. Sharma, M. Feng, Water depollution using metal-organic frameworks-catalyzed advanced oxidation processes: A review, J. Hazard. Mater. 372 (2019) 3–16.

[47] J.-S. Wang, X.-H. Yi, X. Xu, H. Ji, A.M. Alanazi, C.-C. Wang, C. Zhao, Y.V. Kaneti, P. Wang, W. Liu, Y. Yamauchi, Eliminating tetracycline antibiotics matrix via photoactivated sulfate radical-based advanced oxidation process over the immobilized MIL-88A: Batch and continuous experiments, Chem. Eng. J. 431 (2022), 133213.

[48] F.-X. Wang, X.-H. Yi, C.-C. Wang, J.-G. Deng, Photocatalytic Cr(VI) reduction and organic-pollutant degradation in a stable 2D coordination polymer, Chin. J. Catal. 38 (2017) 2141–2149.

[49] Z. Ni, R.I. Masel, Rapid Production of Metal−Organic Frameworks via Microwave-Assisted Solvothermal Synthesis, J. Am. Chem. Soc. 128 (2006) 12394–12395.

[50] O. Abuzalat, D. Wong, M. Elsayed, S. Park, S. Kim, Sonochemical fabrication of Cu (II) and Zn(II) metal-organic framework films on metal substrates, Ultrason. Sonochem. 45 (2018) 180–188.

[51] D. Lv, Y. Chen, Y. Li, R. Shi, H. Wu, X. Sun, J. Xiao, H. Xi, Q. Xia, Z. Li, Efficient Mechanochemical Synthesis of MOF-5 for Linear Alkanes Adsorption, J. Chem. Eng. Data 62 (2017) 2030–2036.

[52] Y. Liu, Y. Wei, M. Liu, Y. Bai, X. Wang, S. Shang, J. Chen, Y. Liu, Electrochemical Synthesis of Large Area Two-Dimensional Metal-Organic Framework Films on Copper Anodes, Angew. Chem. Int. Ed. 60 (2021) 2887–2891.

[53] M. Rubio-Martinez, C. Avci-Camur, A.W. Thornton, I. Imaz, D. Maspoch, M. R. Hill, New synthetic routes towards MOF production at scale, Chem. Soc. Rev. 46 (2017) 3453–3480.

[54] F. Jeremias, S.K. Henninger, C. Janiak, Ambient pressure synthesis of MIL-100 (Fe) MOF from homogeneous solution using a redox pathway, Dalton Trans. 45 (2016) 8637–8644.

[55] H. Fu, X.-X. Song, L. Wu, C. Zhao, P. Wang, C.-C. Wang, Room-temperature preparation of MIL-88A as a heterogeneous photo-Fenton catalyst for degradation of rhodamine B and bisphenol a under visible light, Mater. Res. Bull. 125 (2020), 110806.

[56] Q. Wang, J. Lu, Y. Jiang, S. Yang, Y. Yang, Z. Wang, FeCo bimetallic metal organic framework nanosheets as peroxymonosulfate activator for selective oxidation of organic pollutants, Chem. Eng. J. 443 (2022) 136483.

[57] Y. Ren, S. Wang, J. Zhang, J. Lu, C. Shan, Y. Zhang, D.D. Dionysiou, L. Lv, B. Pan, W. Zhang, Enhancing the performance of Fenton-like oxidation by a dual-layer membrane: A sequential interception-oxidation process, J. Hazard. Mater. 402 (2021) 123766.

[58] T. Araya, M. Jia, J. Yang, P. Zhao, K. Cai, W. Ma, Y. Huang, Resin modified MIL-53 (Fe) MOF for improvement of photocatalytic performance, Appl. Catal. B 203 (2017) 768–777.

[59] T. Araya, C.-C. Chen, M.-K. Jia, D. Johnson, R. Li, Y.-P. Huang, Selective degradation of organic dyes by a resin modified Fe-based metal-organic framework under visible light irradiation, Opt. Mater. 64 (2017) 512–523.

[60] M. Tang, J. Wan, Y. Wang, Z. Yan, Y. Ma, J. Sun, S. Ding, Developing a molecularly imprinted channels catalyst based on template effect for targeted removal of organic micropollutants from wastewaters, Chem. Eng. J. 445 (2022), 136755.

[61] S. Ding, J. Wan, Y. Ma, Y. Wang, X. Li, J. Sun, M. Pu, Targeted degradation of dimethyl phthalate by activating persulfate using molecularly imprinted Fe-MOF-74, Chemosphere 270 (2021) 128620.

[62] S. Ding, J. Wan, Y. Wang, Z. Yan, Y. Ma, Activation of persulfate by molecularly imprinted Fe-MOF-74@SiO2 for the targeted degradation of dimethyl phthalate: Effects of operating parameters and chlorine, Chem. Eng. J. 422 (2021), 130406.

[63] Y. Yao, C. Wang, X. Yan, H. Zhang, C. Xiao, J. Qi, Z. Zhu, Y. Zhou, X. Sun, X. Duan, J. Li, Rational Regulation of Co−N−C Coordination for High-Efficiency Generation of 1O2 toward Nearly 100% Selective Degradation of Organic Pollutants, Environ. Sci. Technol. 56 (2022) 8833–8843.

[64] M. Zhang, C. Xiao, X. Yan, S. Chen, C. Wang, R. Luo, J. Qi, X. Sun, L. Wang, J. Li, Efficient Removal of Organic Pollutants by Metal–organic Framework Derived Co/C Yolk-Shell Nanoreactors: Size-Exclusion and Confinement Effect, Environ. Sci. Technol. 54 (2020) 10289–10300.

[65] Y. Liu, W. Miao, Y. Feng, X. Fang, Q. Li, N. Du, D. Wang, S. Mao, Enhanced peroxydisulfate oxidation via Cu(III) species with a Cu-MOF-derived Cu nanoparticle and 3D graphene network, J. Hazard. Mater. 403 (2021) 123691.

[66] X. Liu, Y. Liu, H. Qin, Z. Ye, X. Wei, W. Miao, D. Yang, S. Mao, Selective Removal of Phenolic Compounds by Peroxydisulfate Activation: Inherent Role of Hydrophobicity and Interface ROS, Environ. Sci. Technol. 56 (2022) 2665–2676.

[67] C. Schweitzer, R. Schmidt, Physical Mechanisms of Generation and Deactivation of Singlet Oxygen, Chem. Rev. 103 (2003) 1685–1758.

[68] Y. Nosaka, A.Y. Nosaka, Generation and Detection of Reactive Oxygen Species in Photocatalysis, Chem. Rev. 117 (2017) 11302–11336.

[69] F.-X. Wang, Z.-C. Zhang, X.-H. Yi, C.-C. Wang, P. Wang, C.-Y. Wang, B. Yu, A micron-sized Co-MOF sheet to activate peroxymonosulfate for efficient organic pollutant degradation, CrstEngComm 24 (2022) 5557–5561.

[70] F. Wang, H. Fu, F.-X. Wang, X.-W. Zhang, P. Wang, C. Zhao, C.-C. Wang, Enhanced catalytic sulfamethoxazole degradation via peroxymonosulfate activation over amorphous CoSx@SiO2 nanocages derived from ZIF-67, J. Hazard. Mater. 423 (2022) 126998.

[71] X.-H. Yi, H. Ji, C.-C. Wang, Y. Li, Y.-H. Li, C. Zhao, A. Wang, H. Fu, P. Wang, X. Zhao, W. Liu, Photocatalysis-activated SR-AOP over PDINH/MIL-88A(Fe) composites for boosted chloroquine phosphate degradation: Performance, mechanism, pathway and DFT calculations, Appl. Catal. B 293 (2021) 120229.

[72] X.-W. Zhang, F. Wang, C.-C. Wang, P. Wang, H. Fu, C. Zhao, Photocatalysis activation of peroxodisulfate over the supported Fe3O4 catalyst derived from MIL-88A(Fe) for efficient tetracycline hydrochloride degradation, Chem. Eng. J. 426 (2021) 131927.

[73] J. Hang, X.-H. Yi, C.-C. Wang, H. Fu, P. Wang, Y. Zhao, Heterogeneous photo-Fenton degradation toward sulfonamide matrix over magnetic Fe3S4 derived from MIL-100(Fe), J. Hazard. Mater. 424 (2022) 127415.

[74] F. Wang, S.-S. Liu, Z. Feng, H. Fu, M. Wang, P. Wang, W. Liu, C.-C. Wang, High-efficient peroxymonosulfate activation for rapid atrazine degradation by FeSx@ MoS2 derived from MIL-88A(Fe), J. Hazard. Mater. 440 (2022) 129723.

[75] Z.-C. Zhang, F.-X. Wang, F. Wang, C.-C. Wang, P. Wang, Efficient atrazine degradation via photoactivated SR-AOP over S-BUC-21(Fe): The formation and contribution of different reactive oxygen species, Sep. Purif. Technol. 307 (2023) 122864.

[76] Y. Li, F. Wang, X. Ren, P. Wang, F.-X. Wang, H.-Y. Chu, S. Gao, C.-C. Wang, Peroxymonosulfate activation for effective atrazine degradation over a 3D cobalt-MOF: Performance and mechanism, J. Environ. Chem. Eng. 11 (2023) 109116.

[77] M. Ahmadi, F. Ghanbari, Degradation of organic pollutants by photoelectro-peroxone/ZVI process: Synergistic, kinetic and feasibility studies, J. Environ. Manage. 228 (2018) 32–39.

[78] J. Cao, Z. Yang, W. Xiong, Y. Zhou, Y. Wu, M. Jia, H. Peng, Y. Yuan, Y. Xiang, C. Zhou, Three-dimensional MOF-derived hierarchically porous aerogels activate peroxymonosulfate for efficient organic pollutants removal, Chem. Eng. J. 427 (2022) 130830.

[79] X. Mi, P. Wang, S. Xu, L. Su, H. Zhong, H. Wang, Y. Li, S. Zhan, Almost 100 % Peroxymonosulfate Conversion to Singlet Oxygen on Single-Atom CoN2+2 Sites, Angew. Chem. Int. Ed. 60 (2021) 4588–4593.

[80] P. Hu, H. Su, Z. Chen, C. Yu, Q. Li, B. Zhou, P.J.J. Alvarez, M. Long, Selective Degradation of Organic Pollutants Using an Efficient Metal-Free Catalyst Derived from Carbonized Polypyrrole via Peroxymonosulfate Activation, Environ. Sci. Technol. 51 (2017) 11288–11296.

[81] X. Duan, H. Sun, Z. Shao, S. Wang, Nonradical reactions in environmental remediation processes: Uncertainty and challenges, Appl. Catal. B 224 (2018) 973–982.

[82] J. Jiang, Z. Zhao, J. Gao, T. Li, M. Li, D. Zhou, S. Dong, Nitrogen Vacancy-Modulated Peroxymonosulfate Nonradical Activation for Organic Contaminant Removal via High-Valent Cobalt-Oxo Species, Environ. Sci. Technol. 56 (2022) 5611–5619.

[83] Y. Zong, X. Guan, J. Xu, Y. Feng, Y. Mao, L. Xu, H. Chu, D. Wu, Unraveling the Overlooked Involvement of High-Valent Cobalt-Oxo Species Generated from the Cobalt(II)-Activated Peroxymonosulfate Process, Environ. Sci. Technol. 54 (2020) 16231–16239.

[84] J. Wei, Z. Xiong, M. Ao, Z. Guo, J. Zhang, B. Lai, Y. Song, Selective degradation of sulfamethoxazole by N-doped iron-based carbon activated peroxymonosulfate: Collaboration of singlet oxygen and high-valent iron-oxo species, Sep. Purif. Technol. 297 (2022) 121379.

[85] T.V. Popova, N.V. Aksenova, Complexes of Copper in Unstable Oxidation States, Russ. J. Coord. Chem. 29 (2003) 743–765.

[86] S. Zhang, T. Hedtke, X. Zhou, M. Elimelech, J.-H. Kim, Environmental Applications of Engineered Materials with Nanoconfinement, ACS ES&T Eng. 1 (2021) 706–724.

[87] A. Al-Anazi, W.H. Abdelraheem, C. Han, M.N. Nadagouda, L. Sygellou, M. K. Arfanis, P. Falaras, V.K. Sharma, D.D. Dionysiou, Cobalt ferrite nanoparticles with controlled composition-peroxymonosulfate mediated degradation of 2-phe-nylbenzimidazole-5-sulfonic acid, Appl. Catal. B 221 (2018) 266–279.

[88] D. Guo, Y. Liu, H. Ji, C.-C. Wang, B. Chen, C. Shen, F. Li, Y. Wang, P. Lu, W. Liu, Silicate-Enhanced Heterogeneous Flow-Through Electro-Fenton System Using Iron Oxides under Nanoconfinement, Environ. Sci. Technol. 55 (2021) 4045–4053.

[89] L. Chen, S. Xu, J. Li, Recent advances in molecular imprinting technology: current status, challenges and highlighted applications, Chem. Soc. Rev. 40 (2011) 2922–2942.

[90] G. Vasapollo, R.D. Sole, L. Mergola, M.R. Lazzoi, A. Scardino, S. Scorrano, G. Mele, Molecularly Imprinted Polymers: Present and Future Prospective, Int. J. Mol. Sci. 12 (2011).

[91] Y. Chen, C.J. Miller, T.D. Waite, Heterogeneous Fenton Chemistry Revisited: Mechanistic Insights from Ferrihydrite-Mediated Oxidation of Formate and Oxalate, Environ. Sci. Technol. 55 (2021) 14414–14425.

[92] W. Wang, Y. Cao, X. Hu, S. Zhou, D. Zhu, D. Qi, S. Deng, Granular reduced graphene oxide/Fe3O4 hydrogel for efficient adsorption and catalytic oxidation of p-perfluoro nonenoxybenzene sulfonate, J. Hazard. Mater. 386 (2020) 121662.

[93] L.N. Pincus, H.E. Rudel, P.V. Petrović, S. Gupta, P. Westerhoff, C.L. Muhich, J. B. Zimmerman, Exploring the Mechanisms of Selectivity for Environmentally Significant Oxo-Anion Removal during Water Treatment: A Review of Common Competing Oxo-Anions and Tools for Quantifying Selective Adsorption, Environ. Sci. Technol. 54 (2020) 9769–9790.

[94] X. Wang, Y. Qin, L. Zhu, H. Tang, Nitrogen-Doped Reduced Graphene Oxide as a Bifunctional Material for Removing Bisphenols: Synergistic Effect between Adsorption and Catalysis, Environ. Sci. Technol. 49 (2015) 6855–6864.

[95] Z. Song, J. Sun, W. Wang, Z. Wang, Y. Zhang, B. Xu, F. Qi, Stable synergistic decontamination and self-cleaning performance of powerful N-rGO catalytic ozonation membrane: Clustering effect of free electrons and role of interface properties, Appl. Catal. B 283 (2021) 119662.

[96] P. Sun, H. Liu, M. Feng, L. Guo, Z. Zhai, Y. Fang, X. Zhang, V.K. Sharma, Nitrogen-sulfur co-doped industrial graphene as an efficient peroxymonosulfate activator: Singlet oxygen-dominated catalytic degradation of organic contaminants, Appl. Catal. B 251 (2019) 335–345.

[97] F. Yang, M. Du, K. Yin, Z. Qiu, J. Zhao, C. Liu, G. Zhang, Y. Gao, H. Pang, Applications of Metal-Organic Frameworks in Water Treatment: A Review, Small 18 (2022) 2105715.

[98] J.-M. Yang, W. Zhang, R.-Z. Zhang, M.-X. Tong, Modulation of the driving forces for adsorption on MIL-101 analogues by decoration with sulfonic acid functional groups: superior selective adsorption of hazardous anionic dyes, Dalton Trans. 49 (2020) 6651–6660.

[99] Y.-H. Li, C.-C. Wang, X. Zeng, X.-Z. Sun, C. Zhao, H. Fu, P. Wang, Seignette salt induced defects in Zr-MOFs for boosted Pb(II) adsorption: universal strategy and mechanism insight, Chem. Eng. J. 442 (2022) 136276.

[100] S. Choi, T. Kim, H. Ji, H.J. Lee, M. Oh, Isotropic and Anisotropic Growth of Metal-Organic Framework (MOF) on MOF: Logical Inference on MOF Structure Based on Growth Behavior and Morphological Feature, J. Am. Chem. Soc. 138 (2016) 14434–14440.

[101] X.-H. Yi, S.-Q. Ma, X.-D. Du, C. Zhao, H. Fu, P. Wang, C.-C. Wang, The facile fabrication of 2D/3D Z-scheme g-C3N4/UiO-66 heterojunction with enhanced photocatalytic Cr(VI) reduction performance under white light, Chem. Eng. J. 375 (2019) 121944.

[102] C. Petit, T.J. Bandosz, MOF–Graphite Oxide Composites: Combining the Uniqueness of Graphene Layers and Metal-Organic Frameworks, Adv. Mater. 21 (2009) 4753–4757.

[103] C. Zhao, Y. Li, H. Chu, X. Pan, L. Ling, P. Wang, H. Fu, C.-C. Wang, Z. Wang, Construction of direct Z-scheme Bi5O7I/UiO-66-NH2 heterojunction photocatalysts for enhanced degradation of ciprofloxacin: Mechanism insight, pathway analysis and toxicity evaluation, J. Hazard. Mater. 419 (2021) 126466.

[104] L. Wu, C.-C. Wang, H.-Y. Chu, X.-H. Yi, P. Wang, C. Zhao, H. Fu, Bisphenol A cleanup over MIL-100(Fe)/CoS composites: Pivotal role of Fe–S bond in regenerating Fe2+ ions for boosted degradation performance, Chemosphere 280 (2021) 130659.

[105] J. Ren, X. Dyosiba, N.M. Musyoka, H.W. Langmi, M. Mathe, S. Liao, Review on the current practices and efforts towards pilot-scale production of metal-organic frameworks (MOFs), Coord. Chem. Rev. 352 (2017) 187–219.

[106] Y.-X. Li, Y.-C. Han, C.-C. Wang, Fabrication strategies and Cr(VI) elimination activities of the MOF-derivatives and their composites, Chem. Eng. J. 405 (2021) 126648.